Published in final edited form as:
Circ Res. 2011 April 29; 108(9): 1042–1052. doi:10.1161/CIRCRESAHA.110.237867.

FKBP12 is a Critical Regulator of the Heart Rhythm and the Cardiac Voltage-Gated Sodium Current in Mice

Mitsunori Maruyama, MD, PhD[*], **Bai-Yan Li, MD, PhD**[*], **Hanying Chen, MD**[*], **Xuehong Xu, PhD**[*], **Long-Sheng Song, MD**, **Wuqiang Zhu, MD, PhD**, **Weidong Yong, PhD**, **Wenjun Zhang, MD**, **Gui-Xue Bu, PhD**, **Shien-Fong Lin, PhD**, **Michael C. Fishbein, MD**, **W. Jonathan Lederer, MD, PhD**, **John H. Schild, Ph.D**, **Loren J. Field, PhD**, **Michael Rubart, MD**, **Peng-Sheng Chen, MD**, and **Weinian Shou, PhD**

Department of Pharmacology (B.-Y.L.), Harbin Medical University; the Krannert Institute for Cardiology and the Division of Cardiology, Department of Medicine (M.M., S.-F.L., L.J.F., P.-S.C.), Riley Heart Research Center, Wells Center for Pediatric Research, Department of Pediatrics (B.-Y.L., H.C., X.X., W.Z., W.Y., W.Z., G-B., L.J.F., M.R.L, W.S.), Indiana University School of Medicine; Medical Biotechnology Center (L.S., W.J.L.), University of Maryland School of Medicine; Division of Anatomical Pathology, Department of Pathology and Laboratory Medicine (M.C.F.), David Geffen School of Medicine, UCLA; Department of Biomedical Engineering (J.H.S.), Purdue School of Engineering and Technology

Abstract

Background—FK506 binding protein 12 (FKBP12) is a known cis-trans peptidyl prolyl isomerase and highly expressed in the heart. Its role in regulating postnatal cardiac function remains largely unknown.

Methods and Results—We generated FKBP12 overexpressing transgenic (αMyHC-FKBP12) mice and cardiomyocyte-restricted FKBP12 conditional knockout ($FKBP12^{f/f}$/αMyHC-Cre) mice, and analyzed their cardiac electrophysiology *in vivo* and *in vitro*. A high incidence (38%) of sudden death was found in αMyHC-FKBP12 mice. Surface and ambulatory ECGs documented cardiac conduction defects, which were further confirmed by electrical measurements and optical mapping in Langendorff-perfused hearts. αMyHC-FKBP12 hearts had slower action potential upstrokes, and longer action potential durations. Whole-cell patch-clamp analyses demonstrated an ~80% reduction in peak density of the tetrodotoxin-resistant, voltage-gated sodium current, I_{Na}, in αMyHC-FKBP12 ventricular cardiomyocytes, a slower recovery of I_{Na} from inactivation, shifts of steady-state activation and inactivation curves of I_{Na} to more depolarized potentials, and augmentation of late I_{Na}, suggesting that the arrhythmogenic phenotype of αMyHC-FKBP12 mice is due to abnormal I_{Na}. Ventricular cardiomyocytes isolated from $FKBP12^{f/f}$/αMyHC-Cre hearts showed faster action potential upstrokes and a more than 2-fold increase in peak I_{Na} density. Dialysis of exogenous recombinant FKBP12 protein into FKBP12-deficient cardiomyocytes promptly recapitulated alterations in I_{Na} seen in αMyHC-FKBP12 myocytes.

Conclusions—FKBP12 is a critical regulator of I_{Na} and is important to cardiac arrhythmogenic physiology. FKPB12-mediated dysregulation of I_{Na} may underlie clinical arrhythmias associated with FK506 administration.

Address correspondence to: Weinian Shou, Riley Heart Research Center, Wells Center for Pediatric Research, Department of Pediatrics, Indiana University School of Medicine.1044 West Walnut, Indianapolis, IN 46202, USA. Phone: (317)274-8952; Fax: (317)274-5378; wshou@iupui.edu.
[*]These authors contributed equally to this work.

Disclosures
There is no disclosure associated with this study.

Keywords

proteins; ion channels; conduction; heart block; long-QT syndrome

Introduction

FK506 binding protein 12 (FKBP12) is a major binding protein for immunosuppressant FK506 and is a 12kDa cis-trans peptidyl prolyl isomerase belonging to the immunophilin family.[1] FKBP12.6, another family member, shares 85% amino acid homology with FKBP12.[2] Despite their close similarity, FKBP12 and FKBP12.6 apparently have different physiological functions.[3, 4] Previously, FKBP12 has been suggested to interact with skeletal muscle calcium release channel ryanodine receptor type 1 (RyR1) and to play an important role in modulating skeletal muscle excitation-contraction coupling,[5] while FKBP12.6 has a much higher affinity to cardiac ryanodine receptor (RyR2) and is more relevant to regulating RyR2 function and calcium release in cardiomyocytes.[2, 6] Mice deficient in FKBP12 exhibit multiple cardiac defects, including ventricular hypertrabeculation, noncompaction and ventricular septal defect, and die *in utero*.[4] Although FKBP12 is indispensable to mammalian cardiac development, its role in the postnatal heart is largely unknown, in spite of the fact that FKBP12 is more abundantly expressed in cardiomyocytes than FKBP12.6.[2, 6, 7]

To investigate the physiological role of FKBP12 in the heart, we created and analyzed cardiomyocyte-restricted FKBP12 conditional knockout ($FKBP12^{f/f}$/αMyHC-Cre) and FKBP12 overexpression transgenic (αMyHC-FKBP12) mice. Our findings provide novel insight of the critical role of FKBP12 in regulating and maintaining heart rhythm via the regulation of voltage-gated Na^+ channels.

Methods

A detailed section is available in the online data supplement.

Generation of Cardiomyocyte-specific FKBP12 Transgenic and Knockout Mice

α-Myosin heavy chain (αMyHC) promoter was placed at 5′ of a human FKBP12 cDNA (Figure 1A). The procedures that generated αMyHC-FKBP12 transgenic mice were carried out as previously described.[8] To achieve spatially and temporally-regulated FKBP12 knockout via the Cre-loxP system, two loxP sites were placed flanking exon 3 of the mouse FKBP12 gene (Figure 5A).

Electrophysiologic and Optical Mapping Study in Langendorff-Perfused Hearts

The heart was perfused with oxygenated Tyrode's solution. Electrophysiologic study was performed with a 2-F octapolar electrode catheter. Transmembrane action potentials (APs) were recorded with standard glass microelectrodes. Optical mapping of voltage-dependent signals was performed using di-4-ANEPPS. Ventricular conduction velocities in the longitudinal (CV_{max}) and transverse (CV_{min}) directions were measured during pacing at the center of the left ventricular lateral wall.[9]

Whole-Cell Patch Techniques

Trans-sarcolemmal currents were recorded using the standard whole-cell patch clamp technique.

Results

Generation of Cardiomyocyte-Restricted FKBP12 Transgenic Mice (αMyHC-FKBP12)

To determine the role of FKBP12 in the heart, we generated αMyHC-FKBP12 transgenic mice (Figure 1A). Three independent transgenic lines (i.e., #4, #6, #12) were generated. Western blot analyses demonstrated that all 3 transgenic lines exhibited about a 9-fold increase in steady state FKBP12 protein levels in the hearts as compared to their non-transgenic controls (Figure 1B). All transgenic mice showed normal development and growth. However, 49 out of 130 αMyHC-FKBP12 transgenic mice (~38%) died suddenly. All three transgenic lines demonstrated similarities in the rates of sudden death and manifestation of electrocardiographic abnormalities (see below). Deaths occurred predominantly between 4–6 weeks of age and were not preceded by any overt signs of illness. There was no sudden death in 151 non-transgenic littermate controls.

At 2 months of age, the heart weight versus body weight ratio in αMyHC-FKBP12 mice was not different from that in non-transgenic littermates. The ventricles of αMyHC-FKBP12 hearts appeared normal grossly and microscopically (Figure 1C). However, the atria of αMyHC-FKBP12 hearts in all three transgenic lines were significantly enlarged compared to non-transgenic littermates at 6–8 weeks of age (Figure 1C). Transthoracic M-mode echocardiography showed that the left ventricular dimensions and contractile function of αMyHC-FKBP12 hearts (n=16) were not significantly altered compared to those of non-transgenic littermates (n=15) (Figure 1D). Interestingly, however, αMyHC-FKBP12 mice in all three transgenic lines exhibited bradyarrhythmias. This unexpected finding suggested the possibility that the sudden deaths in the transgenic mice were caused by cardiac arrhythmias, prompting us to study their electrophysiological phenotype in more detail. As all three transgenic lines gave rise to identical electrocardiographic phenotypes, we mainly used the transgenic line #4 for the following in-depth investigation.

Cardiac Conduction Disturbances in αMyHC-FKBP12 Mice

Surface ECGs recorded from anesthetized αMyHC-FKBP12 mice revealed significantly prolonged PP interval, P wave duration, PQ interval, and QRS duration as compared to non-transgenic mice (Figure 2A, QT intervals were not measured because of difficulty in defining the QT intervals in mice[10]). Eighty-two out of 105 αMyHC-FKBP12 mice studied presented with various degrees of atrioventricular (AV) conduction block. Ambulatory ECG recordings in seven αMyHC-FKBP12 mice demonstrated intermittent complete AV block, whereas AV conduction in five non-transgenic littermates was unaltered (Figure 2B).

To further characterize conduction in αMyHC-FKBP12 hearts, we performed electrophysiological studies in Langendorff-perfused hearts. Compared to non-transgenic littermate controls (n=8), αMyHC-FKBP12 hearts (n=9) had significant prolongations of the AH and HV intervals, the pacing cycle length at which Wenckebach-type AV block occurred, and the effective refractory period of the AV node, indicating depressed intra-atrial, AV and intraventricular conduction (Figure 2C). We also measured conduction velocity in left ventricular epicardium using the optical mapping technique. The conduction velocity in αMyHC-FKBP12 transgenic hearts was significantly slower than that in non-transgenic hearts (Figure 2D), but the degree of conduction anisotropy was not changed. Finally, microelectrode measurements of transmembrane action potentials (AP) from the left ventricular epicardium of isolated hearts revealed deceleration of the maximal phase 0 upstroke velocity [$(dV/dt)_{max}$] and a marked AP prolongation in transgenic hearts (Figure 3A). Taken together, chronic FKBP12 overexpression was associated with abnormal conduction and repolarization.

Altered I_{Na} in αMyHC-FKBP12 Cardiomyocytes

A major determinant of electrical conduction is the magnitude of Na^+ influx through voltage-gated Na^+ channels during the initial fast membrane depolarization.[11] Accordingly, using the whole-cell voltage-clamp technique, we compared the density and properties of the macroscopic voltage-gated Na^+ current (I_{Na}) in αMyHC-FKPB12 and wild-type cardiomyocytes. To avoid the potentially confounding effects of structural abnormalities seen in αMyHC-FKBP12 atria (Figure 1C), current measurements were restricted to ventricular cardiomyocytes. Figure 3B shows representative families of whole-cell I_{Na} in a non-transgenic and anαMyHC-FKBP12 ventricular cardiomyocyte, respectively. Mean peak I_{Na} density was dramatically reduced (~80%) in αMyHC-FKBP12 cardiomyocytes compared to their non-transgenic counterparts, whereas mean whole-cell capacitance was not significantly altered. Peak I_{Na} densities were maximal at −25 mV and −5 mV in wild-type and transgenic myocytes, respectively (Figure 3C). FKBP12 overexpression shifted the peak I_{Na}-V curve to more positive potentials, indicating that the number of Na^+ channels activated at a given membrane voltage was reduced. In addition, we found that recovery of I_{Na} from inactivation was delayed in αMyHC-FKBP12 cardiomyocytes (Figure 3D). Because I_{Na} completely recovered within less than 100 ms in cardiomyocytes of either genotype, the interpulse interval used for measurements of the peak I_{Na}-V relationship (1 s) was sufficient to allow for complete I_{Na} recovery between consecutive voltage pulses. Thus, differences in I_{Na} recovery did not contribute to the reduction in peak I_{Na}. Steady-state I_{Na} activation curves were generated and were fitted by the Boltzmann equation (right two curves in Figure 3E). FKBP12 overexpression caused a positive shift in I_{Na} activation and the slope factor for activation was altered (Supplemental Table I). Steady-state inactivation was determined using a standard double-pulse protocol and the data was fitted by a Boltzmann equation (left two curves in Figure 3E). FKBP12 overexpression resulted in a positive shift in steady-state I_{Na} inactivation, indicating that the fraction of available Na^+ channels at a given membrane potential was increased. The slope factor of steady-state inactivation was not altered. FKBP12 overexpression significantly slowed both the early and late component of I_{Na} inactivation compared with those of wild-type cardiomyocytes (Figure 3F and Supplemental Table II).

TTX inhibition of peak I_{Na} followed single Hill curves with k_d values of 1.2 and 1.6 μM for non-transgenic and transgenic cardiomyocytes, respectively (P>0.05) (Figure 4A). This is consistent with published values of the k_d for the TTX-resistant, i.e. cardiac, I_{Na}.[12] Figure 4B shows that FKBP12 overexpression enhances a persistent and TTX-resistant (3 μM) late I_{Na} component. qRT-PCR, Western blot, and immunofluresence staining demonstrated that $Na_v1.5$, the pore-forming α-subunit of the cardiac, i.e. TTX-resistant, voltage-gate Na^+ channel, was significantly reduced in αMyHC-FKBP12 hearts as compared to non-transgenic hearts, suggesting that the reduction in I_{Na} is partly due to lowered $Na_v1.5$ expression (Figure 4C).

K^+ Currents, L-type Ca^{2+} Currents and $[Ca^{2+}]_i$ Transients in αMyHC-FKBP12 Cardiomyocytes

It has been shown that FK506 has multiple effects on ion channels, which raised the possibility that FKBP12 overexpression also alters other ionic currents. Accordingly, we assessed the voltage-dependence of the inwardly rectifying K^+ current (I_{K1}), the transient outward K^+ current (I_{to}), and sustained K^+ current (I_{Ksus}) in αMyHC-FKBP12 ventricular myocytes. FKBP12 overexpression did not significantly alter I_{K1} and I_{to} densities over the range of membrane potentials tested, while it slightly increased I_{Ksus} density (Supplemental Figure IA). Since increased I_{Ksus} would be expected to shorten APD, we conclude that the APD prolongation observed in αMyHC-FKBP12 cardiomyocytes did not result from altered potassium current densities.

In addition, we simultaneously measured $I_{Ca,L}$ and $[Ca^{2+}]_i$ transients (Supplemental Figure IB). Peak $I_{Ca,L}$ was reduced by 18% in transgenic cells compared to littermate control cells. A decrease in the amplitude of $[Ca^{2+}]_i$ transient was also observed, which seemed to be secondary to changes in $I_{Ca,L}$, due to the similar voltage-dependent reduction in peak amplitudes of $I_{Ca,L}$ and $[Ca^{2+}]_i$. Similarly, a reduction of $I_{Ca,L}$ would be expected to shorten, rather than prolong, APD and thus is not likely to underlie the delay in ventricular repolarization in the transgenic cardiomyocytes.

Generation of Cardiomyocyte-restricted FKBP12 Conditional Knockout Mice

Previously, we have shown that FKBP12-deficient mice exhibit severe defects in cardiac ventricular development and die *in utero*.[4] To determine whether this developmental defect resulted from a cardiomyocyte autonomous origin, we generated FKBP12cardiomyocyte-restricted conditional knockout ($FKBP12^{f/f}$/αMyHC-Cre) mice using the Cre-loxP strategy (Figure 5A). αMyHC-Cre mice were used to ablate FKBP12 in cardiomyocytes. qRT-PCR and Western blot analyses confirmed that FKBP12 was ablated in adult mutant hearts (Figure 5B and 5C). $FKBP12^{f/f}$/αMyHC-Cre mice exhibited normal cardiac development (Figure 6A) and survived to adulthood. Echocardiography showed comparable left ventricular dimensions and contractile function in mutant and littermate control hearts (Figure 6B). Thus, the developmental defects in FKBP12-deficient mice seemed to result from a non-cardiomyocyte origin. This finding was consistent with a previous report by Hamilton and colleague.[13] Importantly, the absence of gross structural abnormalities enabled us to directly assess the effect of FKBP12 deficiency on cardiac electrophysiology, specifically on I_{Na}.

Characterization of I_{Na} in FKBP12-deficient Cardiomyocytes

The surface ECG parameters were not altered between $FKBP12^{f/f}$/αMyHC-Cre mice and $FKBP12^{f/+}$/αMyHC-Cre controls, except for a shorter PP interval in FKBP12-deficient hearts (Figure 6C). No cardiac arrhythmias were observed in $FKBP12^{f/f}$/αMyHC-Cre mice. Left ventricular AP recordings from Langendorff-perfused $FKBP12^{f/f}$/αMyHC-Cre hearts demonstrated a significant acceleration of the maximal phase 0 upstroke velocity compared with $FKBP12^{f/+}$/αMyHC-Cre control hearts (Figure 7A), suggesting an increase in I_{Na} density. Whole-cell voltage-clamp experiments confirmed that the peak I_{Na} density in $FKBP12^{f/f}$/αMyHC-Cre ventricular cardiomyocytes was more than 2-fold larger than that in control cells (Figure 7B). The normalized I_{Na}-V relationships for the $FKBP12^{f/f}$/αMyHC-Cre and control cardiomyocytes were superimposable (Figure 7C), indicating that chronic FKBP12 deficiency did not alter the voltage-dependence of I_{Na} activation (Supplemental Table I). Also, the voltage-dependence of steady-state inactivation and the recovery of I_{Na} from inactivation in $FKBP12^{f/f}$/αMyHC-Cre cardiomyocytes were not different from those in control cardiomyocytes (Figure 7D). Although FKBP12 deficiency accelerated both the early and late component of I_{Na} inactivation (Supplemental Table II), qRT-PCR, Western blot, and immunofluresence staining did not show significant changes in $Na_v1.5$ expression (Figure 7E). Thus, FKBP12 ablation profoundly affected peak I_{Na} density in ventricular cardiomyocytes and altered I_{Na} inactivation gating. In contrast to chronic FKBP12 overexpression, however, FKBP12 deficiency had no detectable effects on other gating properties of cardiac voltage-gated Na^+ channels.

Exogenous FKBP12 Affects I_{Na} in Isolated $FKBP12^{f/f}$/αMyHC-Cre Ventricular Cardiomyocytes

To examine whether FKBP12 acutely regulates voltage-gated Na^+ channels, we performed an *in vitro* experiment wherein $FKBP12^{f/f}$/αMyHC-Cre cardiomyocytes were dialyzed with 1 μg/μl purified recombinant FKBP12 protein through a patch-pipette (Figure 8). The cell was held at −100 mV and stepped from −90 to +30 mV in 5-mV increments from a holding

potential of −100 mV (120 ms pulse duration, 1 s interpulse interval). I_{Na} was recorded repeatedly for a total duration of 60 minutes. Peak I_{Na} progressively declined to a new steady state value during dialysis with exogenous FKBP12 (Figure 8A and C). This phenomenon was not observed in cardiomyocytes dialyzed with control solution without FKBP12 (Figure 8B and C), indicating that the effect of exogenous FKBP12 in the FKBP12-deficient cell resulted from a specific FKBP12-dependent mechanism rather than from I_{Na} run-down (Figure 8C). The shift of the normalized I_{Na}-V plot in FKBP12-reloaded FKPB12$^{f/f}$/αMyHC-Cre myocytes to more positive potentials (Figure 8D), the slowing of I_{Na} decay and rightward shift of both voltage-dependent I_{Na} activation and inactivation (Figure 8E and Supplemental Table III) were similar to those observed in FKBP12-overexpressing cardiomyocytes (Figure 3E). The non-inactivating component of I_{Na} (y_0 in Supplemental Table IV) measured at 45 min was significantly increased compared to that at 5 min, indicating that FKBP12 dialysis augmented a persistent I_{Na}, which is also reflected in an increase in late I_{Na}/peak I_{Na} at the 45-min time point (Figure 8F). Furthermore, action potentials and $(dV/dt)_{max}$ gradually prolongedand decelerated, respectively, over the course of FKPB12 dialysis (Figure 8G and H). Collectively, the relatively fast onset of the effect of exogenous FKBP12 suggests that the changes in I_{Na} density and properties seen in αMyHC-FKBP12 transgenic cardiomyocytes at least partially reflect acute effects of the protein on cardiac voltage-gated Na^+ channels and that FKBP12 protein loading of FKBP12-deficient cardiomyocytes closely replicates the changes in I_{Na} density and channel gating seen in FKBP12 overexpressing myocytes

Discussion

FKBP12 is highly expressed in the heart of diverse vertebrates including mouse and human.[7] However, the role of FKBP12 in postnatal cardiac function remained unclear. The predominant question has been whether FKBP12 plays a role in regulating RyR2. Recent work by Bers and colleagues showed that FKBP12 is unlikely to have any biological impact on RyR2 function.[6] The results of the present study indicate that FKBP12 is critically important in regulating trans-sarcolemmal ionic currents, predominately I_{Na}. This conclusion is based on 1) an increase in peak I_{Na} density in FKBP12-deficient cardiomyocytes, 2) a decrease in peak I_{Na} density, but increase in late I_{Na} density in FKBP12-overexpressed cardiomyocytes; 3) altered I_{Na} inactivation and recovery from inactivation, and shifts of the voltage-dependence of steady-state activation and inactivation to more positive potentials in αMyHC-FKBP12 cardiomyocytes. Importantly, acute delivery of purified FKBP12 protein to FKBP12-null myocytes recapitulated the effects of chronic FKBP12 overexpression on the density and properties of I_{Na}, as well as on the duration and phase 0 $(dV/dt)_{max}$ of the action potential, indicating that the effect of FKBP12 did not arise due to unspecific structural and/or functional alterations.

Loss-of-function mutations in SCN5a gene encoding $Na_v1.5$ lead to cardiac arrhythmias, including progressive cardiac conduction defects,[14] sick sinus syndrome,[15] and Brugada syndrome,[16] while gain-of-function mutations lead to type 3 long QT syndrome.[17] Combinatorial phenotypes have been reported in patients with SCN5a mutations causing both reduced peak I_{Na} and increased late I_{Na}.[18] Suppression of peak I_{Na} can result in cardiac conduction disturbance[19] and abnormal sinus node function,[20] whereas increased late I_{Na} reduces repolarization reserve and prolongs APD which can induce early afterdepolarizations, triggered arrhythmias, and sudden cardiac death.[21] Cardiac overexpression of FKBP12 recapitulated many of the phenotypic abnormalities seen in patients with SCN5a mutations. Interestingly, the immunosuppressant FK506 has been shown to adversely affect cardiac electrophysiology, causing long QT syndrome, sinus arrest, and sudden death in patients treated with FK506.[22–28] This adverse effect was similarly demonstrated in guinea pigs.[29, 30] Bers and colleagues observed an increase in

APD in FK506-treated cardiomyocytes.[31] These previous observations along with our data hint a potential role of FKBP12-mediated dysregulation of I_{Na} as the mechanism underlying FK506-induced clinical arrhythmias.

The ionic mechanisms underlying the AV conduction abnormalities in αMyHC-FKBP12 mice may also involve downregulation of $I_{Ca,L}$, a major determinant of conduction across the AV junction.[32] The mechanisms of $I_{Ca,L}$ downregulation is unclear and awaits further study. Reduction in both phase 0 $(dV/dt)_{max}$ and ventricular conduction velocity at near physiological rates (Figures 2 and 3) strongly supports the notion that the electrocardiographic manifestations of impaired ventricular conduction directly result from FKBP12 overexpression-induced reduction in net Na^+ influx through activated voltage-gated Na^+ channels during the initial fast depolarization of the AP. In contrast, the involvement of I_{Na} in mediating APD prolongation inαMyHC-FKBP12 ventricular cardiomyocytes is less clear. Slowed I_{Na} inactivation and the positive shift of the I_{Na} steady-state inactivation curve would be expected to synergistically augment Na^+ influx, increasing net inward current during the repolarizing phases of the ventricular AP, whereas the reduction in I_{Na} density, slowing of I_{Na} recovery, and the positive shift of the activation curve would be expected to exert the opposite effect. Although our measurements clearly demonstrate a marked increase in a persistent TTX-insensitive current in αMyHC-FKBP12 ventricular cardiomyocytes, it remains to be seen whether this phenomenon is solely responsible for the marked APD elongation. The observation that FKBP12 overexpression is associated with a reduction in $I_{Ca.L}$ and increases in I_{Ksus} (both of which would shorten the AP) suggests that, by exclusion, I_{Na} underlies delayed repolarization.

It is somewhat puzzling that genetic FKBP12 ablation, in contrast to FKBP12 overexpression, only affects peak I_{Na} density and I_{Na} inactivation kinetics, but does not significantly alter voltage-dependence of I_{Na} activation and inactivation, or I_{Na} recovery from inactivation compared with wild-type myocytes. This may reflect the presence of multiple regulatory mechanisms with different FKBP12 sensitivities. For example, baseline levels of FKBP12 appear to be sufficient to control the number of functional channels in the sarcolemma, and to regulate I_{Na} inactivation kinetics. In contrast, higher levels of the protein seem to be required to achieve a noticeable effect on voltage-dependence of I_{Na} activation and inactivation. It would be interesting to examine whether FKBP12 expression is significantly altered in the diseased heart, causing changes in excitability and conduction.

The main cardiac voltage-gated Na^+ channel consists of a $Na_v1.5$ α-subunit and an ancillary β-subunit. In addition, a series of channel modulators and regulators are important to its function.[33] Our work suggests that FKBP12 is an important regulator of cardiac voltage-gated Na^+ channels, although the exact biochemical nature that underlies the FKBP12-channel interaction remains unclear. The reduction of the peak I_{Na} density in αMyHC-FKBP12 transgenic likely results from a combination of reduced $Na_v1.5$ protein expression and posttranslational modification of the sodium channel protein complex. The marked changes in the biophysical properties of I_{Na} in FKBP12-deficient and transgenic cardiomyocytes suggest that FKBP12 acts directly (via protein-protein interaction) or indirectly (via modulation of 2nd messenger pathways) to modulate I_{Na}. Co-immunoprecipitation and pull-down assays failed to demonstrate direct interaction between FKBP12 and $Na_v1.5$ (data not shown), suggesting that some intermediate protein(s) is (are) mediating the interaction between FKBP12 and channel proteins. Further work is needed to identify the detailed molecular mechanism of FKBP12-channel protein interaction. In conclusion, by analyzing genetically modified mouse models, we demonstrate for the first time that FKBP12 is important for normal physiological function of the cardiac voltage-gated Na^+ channel, and is relevant to cardiac arrhythmogenesis.

Supplementary Material

Refer to Web version on PubMed Central for supplementary material.

Acknowledgments

We wish to thank Dr. Shaoliang Jing and Mr. William Carter of Indiana University mouse core for their superb assistance in generating these mutant mice.

Sources of Funding

This study was supported by the NIH Grants NIH R01-HL70259 (Shou) and P01 HL85098 (Shou, Field), R01-HL 75165 (Rubart), and P01 HL78931, R01 HL78932 and 71140 (Chen), Nihon Kohden / St. Jude Medical Electrophysiology fellowship (Maruyama), the Piansky FamilyTrust (Fishbein) and the Medtronic-Zipes Endowments (Chen).

Non-standard abbreviations and acronyms

AH	atrial-His
αMyHC-Cre	alpha myosin heavy chain promoter-Cre transgenic mice
AP	action potential
APD	action potential duration
AV	atrioventricular
CV	conduction velocity
ECG	electrocardiogram
EF%	ejection fraction
AVN-ERP	effective refractory period of the atrioventricular node
FKBP12	FK506 Binding Protein 12
FKBP12.6	FK506 Binding Protein 12.6
FS%	fractional shortening
HV	His-ventricular
$I_{Ca,L}$	L-type Ca^{2+} current
I_{K1}	inward rectifying K^+ current
I_{to}	transient outward K^+ current
I_{Ksus}	sustained K^+ current
I_{Na}	voltage-gated Na^+ current
$Na_v1.5$	cardiac voltage-gated sodium channel pore forming alpha subunit
LVIDd	end-diastolic left ventricular internal diameter
LVIDs	end-systolic left ventricular internal diameter
LVvold	end-diastolic left ventricular volume
LVvols	end-systolic left ventricular volume
NTG	non-transgenic
RyR1	ryanodine receptor type 1

RyR2	ryanodine receptor type 2
SCN5a	the human gene encoding the voltage-gated sodium channel alpha subunit $Na_v1.5$
TG	transgenic
Tie2-Cre	angiopoietin receptor 2 promoter -Cre transgenic mice
TTX	tetrodotoxin
WCL	Wenckebach cycle length
WT	wild type

References

1. Snyder SH, Sabatini DM. Immunophilins and the nervous system. Nature medicine. 1995; 1:32–37.
2. Timerman AP, Onoue H, Xin HB, Barg S, Copello J, Wiederrecht G, Fleischer S. Selective binding of FKBP12.6 by the cardiac ryanodine receptor. The Journal of biological chemistry. 1996; 271:20385–20391. [PubMed: 8702774]
3. Xin HB, Senbonmatsu T, Cheng DS, Wang YX, Copello JA, Ji GJ, Collier ML, Deng KY, Jeyakumar LH, Magnuson MA, Inagami T, Kotlikoff MI, Fleischer S. Oestrogen protects FKBP12.6 null mice from cardiac hypertrophy. Nature. 2002; 416:334–338. [PubMed: 11907581]
4. Shou W, Aghdasi B, Armstrong DL, Guo Q, Bao S, Charng MJ, Mathews LM, Schneider MD, Hamilton SL, Matzuk MM. Cardiac defects and altered ryanodine receptor function in mice lacking FKBP12. Nature. 1998; 391:489–492. [PubMed: 9461216]
5. Marx SO, Ondrias K, Marks AR. Coupled gating between individual skeletal muscle Ca2+ release channels (ryanodine receptors). Science. 1998; 281:818–821. [PubMed: 9694652]
6. Guo T, Cornea RL, Huke S, Camors E, Yang Y, Picht E, Fruen BR, Bers DM. Kinetics of FKBP12.6 binding to ryanodine receptors in permeabilized cardiac myocytes and effects on ca sparks. Circ Res. 2010; 106:1743–1752. [PubMed: 20431056]
7. Jeyakumar LH, Ballester L, Cheng DS, McIntyre JO, Chang P, Olivey HE, Rollins-Smith L, Barnett JV, Murray K, Xin HB, Fleischer S. FKBP binding characteristics of cardiac microsomes from diverse vertebrates. Biochem Biophys Res Commun. 2001; 281:979–986. [PubMed: 11237759]
8. Chen H, Yong W, Ren S, Shen W, He Y, Cox KA, Zhu W, Li W, Soonpaa M, Payne RM, Franco D, Field LJ, Rosen V, Wang Y, Shou W. Overexpression of bone morphogenetic protein 10 in myocardium disrupts cardiac postnatal hypertrophic growth. J Biol Chem. 2006; 281:27481–27491. [PubMed: 16798733]
9. Gutstein DE, Morley GE, Tamaddon H, Vaidya D, Schneider MD, Chen J, Chien KR, Stuhlmann H, Fishman GI. Conduction slowing and sudden arrhythmic death in mice with cardiac-restricted inactivation of connexin43. Circulation research. 2001; 88:333–339. [PubMed: 11179202]
10. Danik S, Cabo C, Chiello C, Kang S, Wit AL, Coromilas J. Correlation of repolarization of ventricular monophasic action potential with ECG in the murine heart. American journal of physiology. 2002; 283:H372–381. [PubMed: 12063311]
11. Kleber AG, Rudy Y. Basic mechanisms of cardiac impulse propagation and associated arrhythmias. Physiol Rev. 2004; 84:431–488. [PubMed: 15044680]
12. Goldin AL. Resurgence of sodium channel research. Annu Rev Physiol. 2001; 63:871–894. [PubMed: 11181979]
13. Tang W, Ingalls CP, Durham WJ, Snider J, Reid MB, Wu G, Matzuk MM, Hamilton SL. Altered excitation-contraction coupling with skeletal muscle specific FKBP12 deficiency. FASEB J. 2004; 18:1597–1599. [PubMed: 15289441]
14. Schott JJ, Alshinawi C, Kyndt F, Probst V, Hoorntje TM, Hulsbeek M, Wilde AA, Escande D, Mannens MM, Le Marec H. Cardiac conduction defects associate with mutations in SCN5A. Nature genetics. 1999; 23:20–21. [PubMed: 10471492]

15. Benson DW, Wang DW, Dyment M, Knilans TK, Fish FA, Strieper MJ, Rhodes TH, George AL Jr. Congenital sick sinus syndrome caused by recessive mutations in the cardiac sodium channel gene (SCN5A). J Clin Invest. 2003; 112:1019–1028. [PubMed: 14523039]

16. Brugada J, Brugada R, Brugada P. Channelopathies: a new category of diseases causing sudden death. Herz. 2007; 32:185–191. [PubMed: 17497250]

17. Wang Q, Shen J, Splawski I, Atkinson D, Li Z, Robinson JL, Moss AJ, Towbin JA, Keating MT. SCN5A mutations associated with an inherited cardiac arrhythmia, long QT syndrome. Cell. 1995; 80:805–811. [PubMed: 7889574]

18. Remme CA, Wilde AA, Bezzina CR. Cardiac sodium channel overlap syndromes: different faces of SCN5A mutations. Trends Cardiovasc Med. 2008; 18:78–87. [PubMed: 18436145]

19. Shaw RM, Rudy Y. Ionic mechanisms of propagation in cardiac tissue. Roles of the sodium and L-type calcium currents during reduced excitability and decreased gap junction coupling. Circulation Research. 1997; 81:727–741. [PubMed: 9351447]

20. Butters TD, Aslanidi OV, Inada S, Boyett MR, Hancox JC, Lei M, Zhang H. Mechanistic Links Between Na+ Channel (SCN5A) Mutations and Impaired Cardiac Pace making in Sick Sinus Syndrome. Circ Res. 2010; 107:126–137. [PubMed: 20448214]

21. Nuyens D, Stengl M, Dugarmaa S, Rossenbacker T, Compernolle V, Rudy Y, Smits JF, Flameng W, Clancy CE, Moons L, Vos MA, Dewerchin M, Benndorf K, Collen D, Carmeliet E, Carmeliet P. Abrupt rate accelerations or premature beats cause life-threatening arrhythmias in mice with long-QT3 syndrome. Nat Med. 2001; 7:1021–1027. [PubMed: 11533705]

22. Calandra S. Sinus arrest during tacrolimus treatment: was the QT interval prolonged? Transplantation. 1998; 66:402–404. [PubMed: 9721813]

23. Cox TH, Baillie GM, Baliga P. Bradycardia associated with intravenous administration of tacrolimus in a liver transplant recipient. Pharmacotherapy. 1997; 17:1328–1330. [PubMed: 9399620]

24. Hodak SP, Moubarak JB, Rodriguez I, Gelfand MC, Alijani MR, Tracy CM. QT prolongation and near fatal cardiac arrhythmia after intravenous tacrolimus administration: a case report. Transplantation. 1998; 66:535–537. [PubMed: 9734501]

25. Johnson MC, So S, Marsh JW, Murphy AM. QT prolongation and Torsades de Pointes after administration of FK506. Transplantation. 1992; 53:929–930. [PubMed: 1373538]

26. Minematsu T, Ohtani H, Sato H, Iga T. Pharmacokinetic/pharmacodynamic analysis of tacrolimus-induced QT prolongation in guinea pigs. Biological & pharmaceutical bulletin. 1999; 22:1341–1346. [PubMed: 10746167]

27. Sawabe T, Mizuno S, Gondo H, Maruyama T, Niho Y. Sinus arrest during tacrolimus (FK506) and digitalis treatment in a bone marrow transplant recipient. Transplantation. 1997; 64:182–183. [PubMed: 9233725]

28. Akers WS, Flynn JD, Davis GA, Green AE, Winstead PS, Strobel G. Prolonged cardiac repolarization after tacrolimus and haloperidol administration in the critically ill patient. Pharmacotherapy. 2004; 24:404–408. [PubMed: 15040655]

29. Minematsu T, Ohtani H, Sato H, Iga T. Sustained QT prolongation induced by tacrolimus in guinea pigs. Life sciences. 1999; 65:PL197–202. [PubMed: 10530807]

30. Minematsu T, Ohtani H, Yamada Y, Sawada Y, Sato H, Iga T. Quantitative relationship between myocardial concentration of tacrolimus and QT prolongation in guinea pigs: pharmacokinetic/pharmacodynamic model incorporating a site of adverse effect. Journal of pharmacokinetics and pharmacodynamics. 2001; 28:533–554. [PubMed: 11999291]

31. McCall E, Li L, Satoh H, Shannon TR, Blatter LA, Bers DM. Effects of FK-506 on contraction and Ca2+ transients in rat cardiac myocytes. Circulation research. 1996; 79:1110–1121. [PubMed: 8943949]

32. Katz AM. Calcium channel diversity in the cardiovascular system. J Am Coll Cardiol. 1996; 28:522–529. [PubMed: 8800134]

33. Abriel H, Kass RS. Regulation of the voltage-gated cardiac sodium channel Nav1.5 by interacting proteins. Trends Cardiovasc Med. 2005; 15:35–40. [PubMed: 15795161]

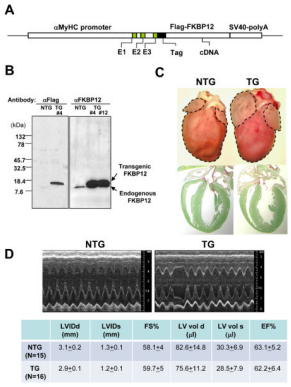

	LVIDd (mm)	LVIDs (mm)	FS%	LV vol d (μl)	LV vol s (μl)	EF%
NTG (N=15)	3.1±0.2	1.3±0.1	58.1±4	82.6±14.8	30.3±6.9	63.1±5.2
TG (N=16)	2.9±0.1	1.2±0.1	59.7±5	75.6±11.2	28.5±7.9	62.2±6.4

Figure 1.

αMyHC-FKBP12 transgenic mice. A, Schematic diagram of the αMyHC-FKBP12 transgene construct. B, Western blot analysis of transgenic FKBP12 expression in cardiac tissues from αMyHC-FKBP12 transgenic mice (TG, transgenic line #4 and #12 as indicated) and non-transgenic controls (NTG). The endogenous FKBP12 and the overexpressed transgenic FKBP12 are indicated by arrows. C, Comparison of cardiac morphology of NTG and TG hearts (6-week old). Histological sections were stained with fast green and sirius red (lower panels). TG heart exhibited biatrial enlargement. D, Representative M-mode echocardiograms in a NTG and TG mouse. TG hearts exhibited normal left ventricular dimensions and contractile performance, but the heart rate was slower and irregular. LVIDd and LVIDs indicate end-diastolic and end-systolic left ventricular internal dimensions, respectively; FS%, fractional shortening; LVvol d and LVvol s, end-diastolic and end-systolic left ventricular volumes, respectively; EF%, ejection fraction.

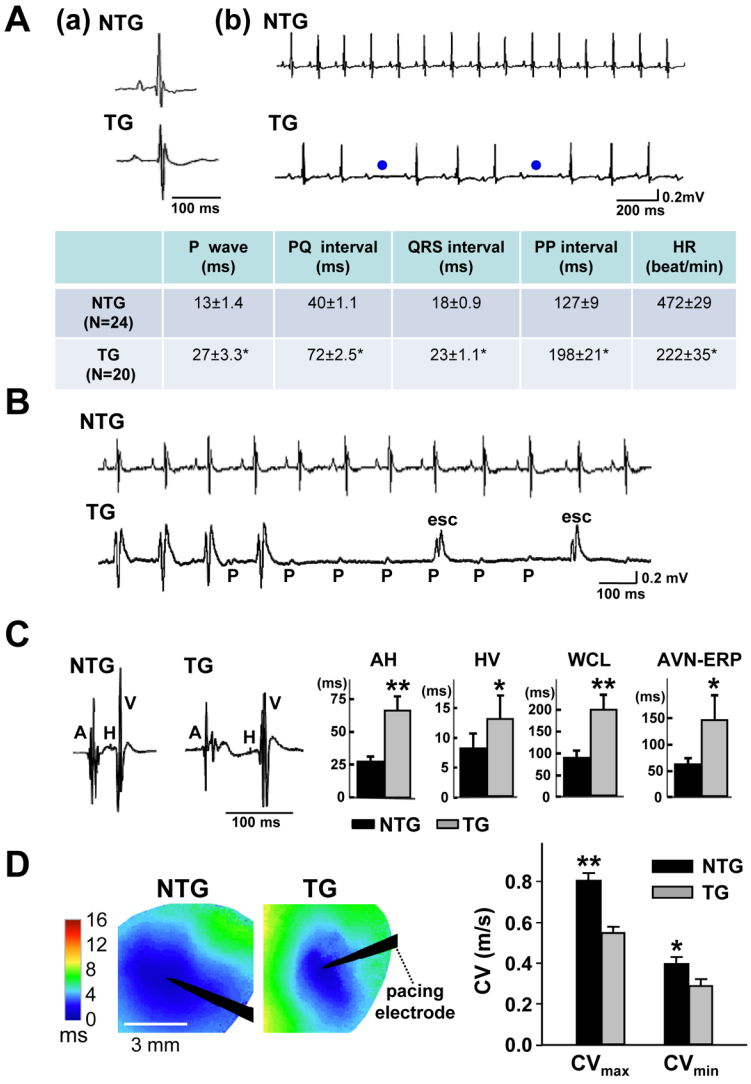

	P wave (ms)	PQ interval (ms)	QRS interval (ms)	PP interval (ms)	HR (beat/min)
NTG (N=24)	13±1.4	40±1.1	18±0.9	127±9	472±29
TG (N=20)	27±3.3*	72±2.5*	23±1.1*	198±21*	222±35*

Figure 2.

Adult αMyHC-FKBP12 mice exhibit abnormal cardiac conduction and rhythm. **A**, (a and b) Representative surface ECGs obtained from a NTG and a TG mouse, respectively. The ECG from the TG mouse shows longer PP intervals and 2nd degree AV block (blue dots). Table summarizes the ECG parameters obtained in TG (n=20) and NTG mice (n=24); **P*<0.001 for TG versus NTG. **B**, Representative ambulatory ECG tracings in conscious NTG and TG mice. Transient complete AV block with escape rhythm (esc) was observed in the TG mouse**. C**, Electrophysiological analysis in Langendorff-perfused hearts. The left two panels show representative intracardiac electrograms recorded in an NTG and TG heart, respectively. Bar graphs show that the means for the AH (atrium-His) and HV (His-ventricular) intervals, Wenckebach cycle length (WCL), and effective refractory period of the AV node (AVN-ERP) were significantly prolonged in TG hearts (TG: n=9; NTG: n=8); **P*<0.05; ***P*<0.01 for TG versus NTG. **D**, Left ventricular epicardial conduction velocities (CVs) (TG: n=7; NTG: n=7). Left panels illustrate representative color-coded isochronal maps during unipolar pacing. Black arrow heads denote positions of stimulating electrodes. The mean CVs in TG hearts were significantly smaller in both the longitudinal and transverse direction compared with the NTG hearts. **P*<0.05; ***P*<0.01.

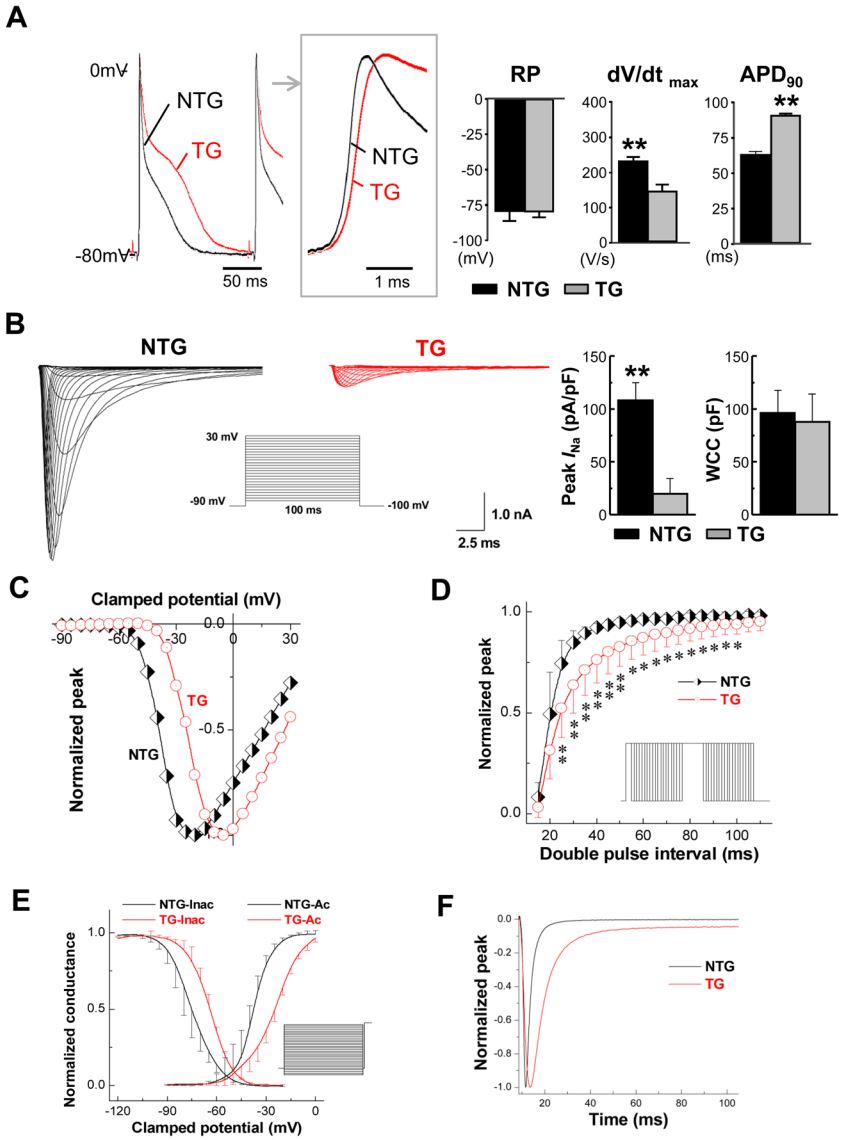

Figure 3.

Cellular electrophysiology of αMyHC-FKBP12 ventricular cardiomyocytes. **A**, Representative ventricular transmembrane APs recorded from isolated TG and NTG hearts. Box shows the initial portions of the respective APs at an expanded time scale. On average, maximum upstroke velocity of phase 0 of the AP [$(dV/dt)_{max}$] was decreased in TG hearts (n=7) compared to NTG hearts (n=6), despite similar mean resting membrane potentials (RP). Significantly longer APD at 90% repolarization (APD_{90}) was noted in TG hearts. $^{**}P<0.01$ for NTG versus TG. APs were recorded at a pacing cycle length of 150 ms. **B–F**, Voltage-clamp analysis of macroscopic I_{Na} in ventricular cardiomyocytes isolated from TG (n=14 cells/4 hearts) and NTG (n=14 cell/4 hearts) hearts. **B**, Representative I_{Na} traces elicited by 120 ms depolarizing pulses to potentials from −90 to +30 mV from a holding potential of −100 mV at 5-mV increments (interpulse interval, 1 s). Insert shows schematic of the voltage-clamp protocol. Bar graphs in B show means ± SD of maximal peak I_{Na} densities measured at −5 mV and −25 mV in TG and NTG myocytes, respectively, and whole cell capacitance (WCC), $^{**}P<0.01$. **C**, Normalized I_{Na}-V plots. Values for peak I_{Na} density at each voltage were normalized to their respective maximal peak I_{Na} density at −25

mV (NTG) and −5 mV (TG) and plotted as a function of voltage. **D**, FKBP12 overexpression slows I_{Na} recovery from inactivation. Insert shows schematic voltage-clamp protocol. *P<0.05 and **P<0.01 versus NTG. **E**, Voltage-dependence of steady-state I_{Na} activation (right curves) and inactivation (left curves). **F**, Time course of I_{Na} in an αMyHC-FKBP12 (red) and a non-transgenic ventricular cardiomyocyte.

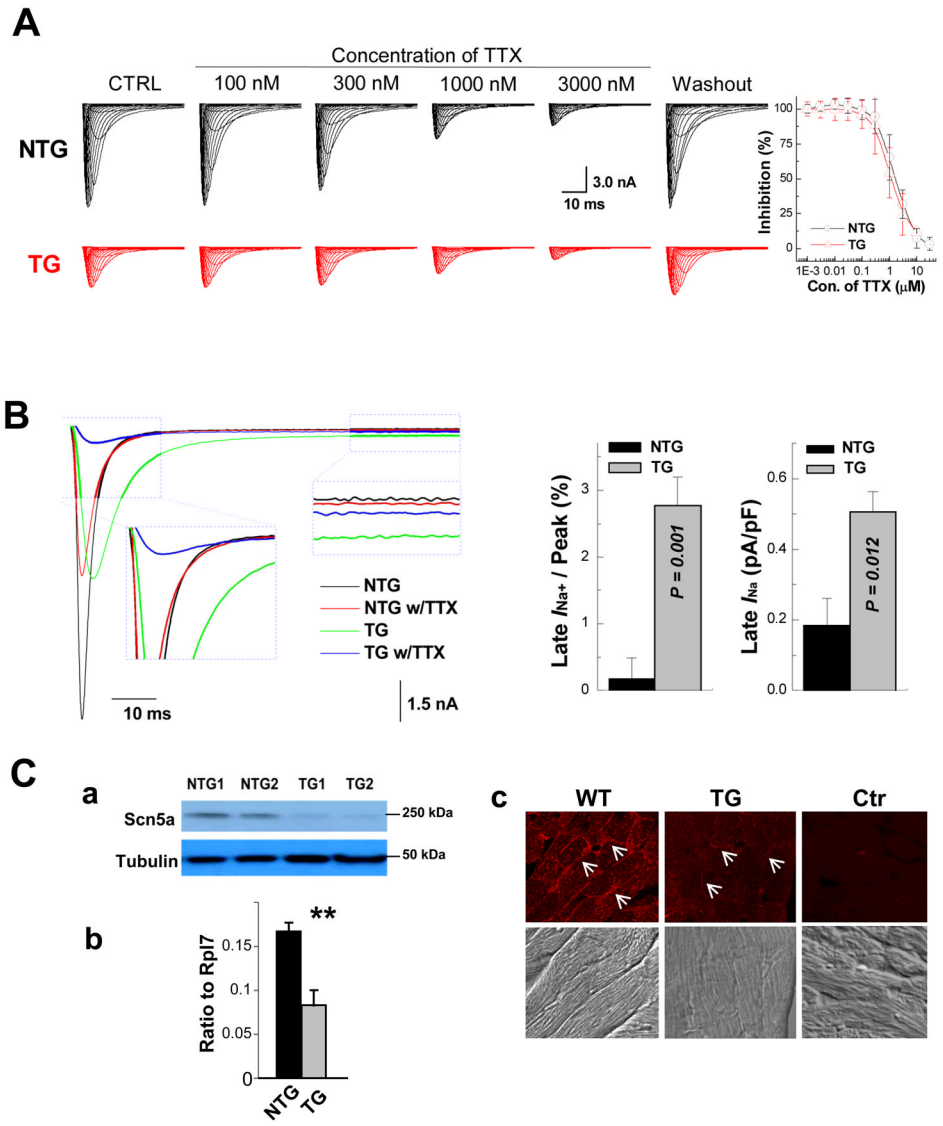

Figure 4.

Assessment of late I_{Na}. **A**, Ventricular cardiomyocytes from αMyHC-FKBP12 and wild-type mice express the TTX-resistant (cardiac-isoform) but not TTX-sensitive (neuronal-isoforms) of voltage-gated Na^+ channels. (Left panels) Representative I_{Na} responses to increasing concentrations of extracellular TTX in TG and NTG ventricular cardiomyocytes. (Right panel) Plots of the percent inhibition of peak I_{Na} as a function of TTX concentration in transgenic (n=4) and non-transgenic (n=3) myocytes. Mean Hill coefficients for TTX-block of peak I_{Na} were 1.2 and 1.3 (P>0.05) for the NTG and TG cardiomyocytes, suggesting that a single TTX molecule blocks a single Na^+ channel. Nanomolar concentrations of TTX that typically block neuronal-isoforms of voltage-gated Na^+ channels had no detectable effect on peak I_{Na} in either cardiomyocyte-type. **B**, FKBP12 overexpression enhances a persistent Na^+ current. Original traces of I_{Na} elicited from −100 mV to +30 mV for 400 ms before and after exposure to 3 μM TTX in the external solution. TTX-sensitive components were averaged over the last 100 ms of the depolarizing pulse and normalized to the cell capacitance. FKBP12 overexpression increased mean late I_{Na} density (P<0.05). C, Assessment of $Na_v1.5$ expression and cellular localization. Western blot (a),

qRT-PCR (b), and immunofluorescence and confocal imaging (c) analyses demonstrated a significant reduction of $Na_v1.5$ in transgenic hearts. Confocal images were representative for three independent sets of experiment. White arrows (in c) denote anti-Nav1.5 immune reactivity in the outer surface membrane of cardiomyocytes. $^{**}P < 0.01$.

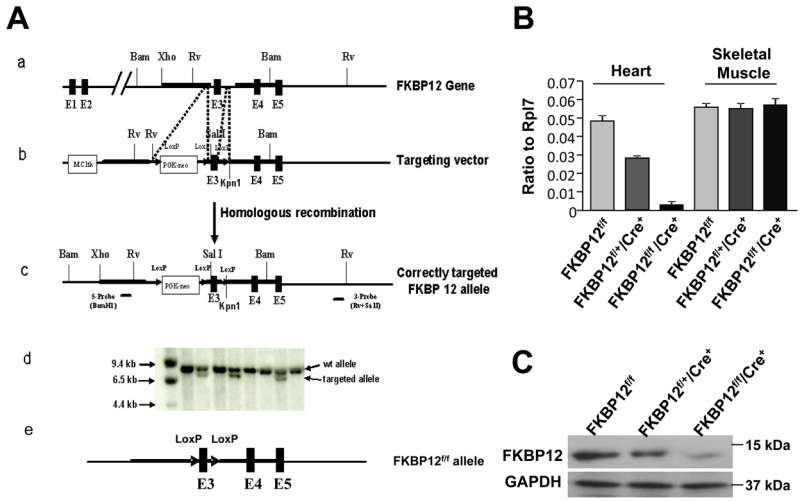

Figure 5.

Generation of FKBP12 conditional knockout using Cre-loxP system. A, (a-c) Targeting vector to mutate the mouse FKBP12 gene with PGK-neo cassette and loxP sites ($FKBP12^{loxP\text{-}neo}$). (d) Southern blot analysis of targeted ES cells. (e) Removal of PGKneo-loxP cassette from $FKBP12^{loxP\text{-}neo}$ mice. This was achieved by taking advantage of maternal expression of Cre in oocytes of Tie2-Cre transgenic females, as the oocytes have a transient presence of Cre protein from maternal Cre-mRNA. Using a PCR based genotyping strategy for PGK-Neo negative and Exon 3-loxP positive offspring, we were able to generate mice that contain only a single pair of loxP sites flanking exon 3 in FKBP12 allele ($FKBP12^{flox}$). B and C, Assessment of efficiency of FKBP12 ablation using αMyHC-Cre. B, qRT-PCR analysis to determine the level of FKBP12 transcript in heart and skeletal muscle samples with indicated genotypes. C, Western blot analysis to determine the FKBP12 protein level in hearts. FKBP12 is efficiently removed from cardiac tissues in $FKBP12^{f/f}$/αMyHC-Cre hearts.

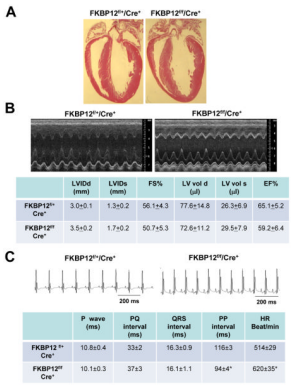

	LVIDd (mm)	LVIDs (mm)	FS%	LV vol d (µl)	LV vol s (µl)	EF%
FKBP12f/+ Cre+	3.0±0.1	1.3±0.2	56.1±4.3	77.6±14.8	26.3±6.9	65.1±5.2
FKBP12f/f Cre+	3.5±0.2	1.7±0.2	50.7±5.3	72.6±11.2	29.5±7.9	59.2±6.4

	P wave (ms)	PQ interval (ms)	QRS interval (ms)	PP interval (ms)	HR Beat/min
FKBP12 f/+ Cre+	10.8±0.4	33±2	16.3±0.9	116±3	514±29
FKBP12f/f Cre+	10.1±0.3	37±3	16.1±1.1	94±4*	620±35*

Figure 6.

Cardiomyocyte-restricted conditional knockout hearts (FKBP12$^{f/f}$/αMyHC-Cre^{+}) **A**, Histological sections with H&E staining show normal development and structure of FKBP12$^{f/f}$/αMyHC-Cre^{+} and littermate control (FKBP12$^{f/+}$/αMyHC-Cre^{+}) hearts. **B**, M-mode echocardiograms from an FKBP12$^{f/f}$/αMyHC-Cre^{+} and a control FKBP12$^{f/+}$/αMyHC-Cre^{+} mouse show normal dimensions and contractile function of the left ventricles. **C**, Representative surface ECGs recorded from an FKBP12$^{f/+}$/αMyHC-Cre^{+} and an FKBP12$^{f/f}$/αMyHC-Cre^{+} mouse. The mean heart rate (HR) was significantly higher in the FKBP12-deficient mice (n=10) compared with FKBP-expressing mice (n=10), **P*<0.05.

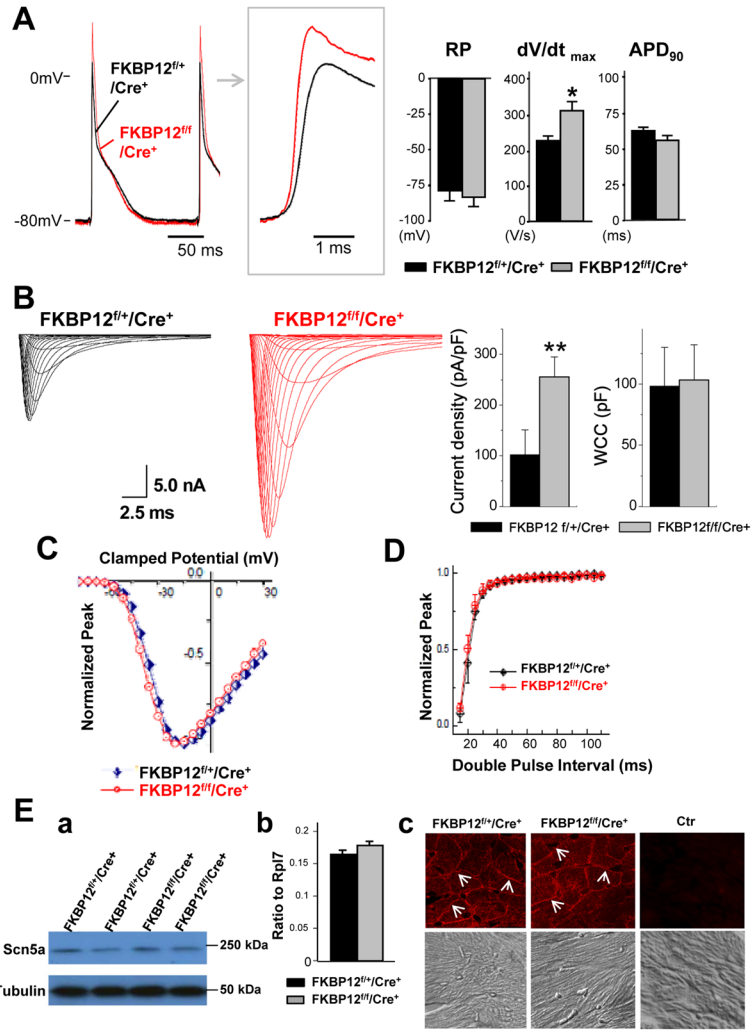

Figure 7.

Cellular electrophysiological analyses of FKPB12$^{f/f}$/αMyHC-Cre^{+} and FKBP12$^{f/+}$/αMyHC-Cre^{+} hearts. **A**, Representative ventricular transmembrane APs recorded from an FKBP12$^{f/f}$/αMyHC-Cre^{+} and an FKBP12$^{f/+}$/αMyHC-Cre^{+} heart. Maximum upstroke velocity of phase 0 of the AP $(dV/dt)_{max}$ and peak action potential amplitude were increased in FKBP12$^{f/f}$/αMyHC-Cre^{+} hearts compared to control hearts (n=4 in both groups). The means of RP and APD_{90} were similar between FKBP12$^{f/f}$/Cre^{+} and FKBP12$^{f/+}$/Cre^{+} hearts. *P<0.05. **B**, I_{Na} traces recorded from isolated FKBP12$^{f/f}$/αMyHC-Cre^{+} and control FKBP12$^{f/+}$/αMyHC-Cre^{+} ventricular cardiomyocytes. The maximal peak I_{Na} in FKBP12$^{f/f}$/αMyHC-Cre^{+} myocytes (n=30 cells/8 hearts) was increased by more than 2.5-fold compared to FKBP12$^{f/+}$/αMyHC-Cre^{+} cells (n=15 cells/6 hearts). **P<0.01. **C**, Normalized peak I_{Na}-V relationships. **D**, I_{Na} recovery from inactivation. **E,** Assessment of $Na_v1.5$ expression and cellular localization using Western blot (a), qRT-PCR (b), and immunofluorescence and confocal imaging (c). The level of $Na_v1.5$ expression was not significantly altered. Immunofluorescence confocal images were representative for three independent sets of experiment. White arrows (in c) denote anti-Nav1.5 immune reactivity in the outer membranes of cardiomyocytes.

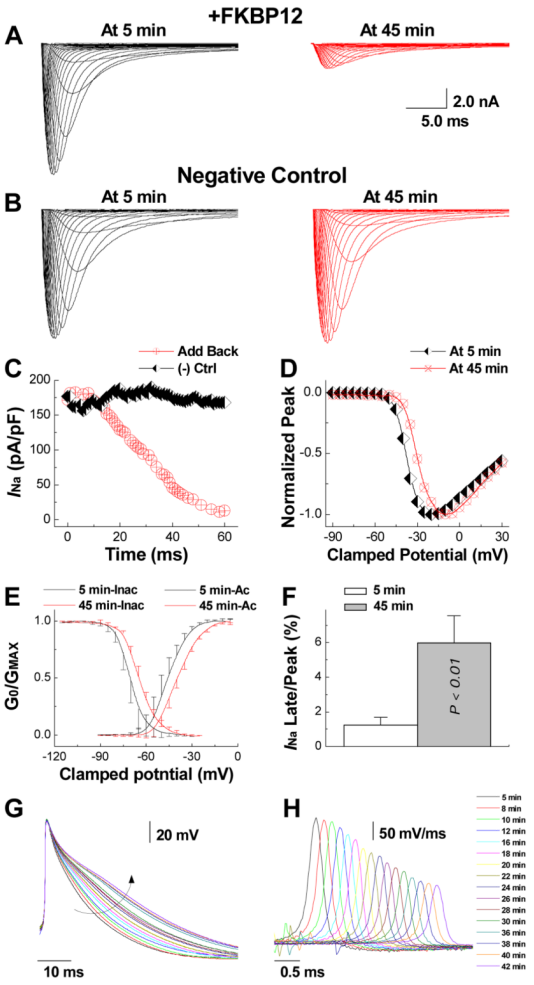

Figure 8.

Direct delivery of exogenous FKBP12 protein into FKBP12$^{f/f}$/αMyHC-Cre^{+} ventricular cardiomyocytes replicates the effects of chronic FKBP12 overepxression on I_{Na} density and gating. **A**, Representative I_{Na} traces obtained from an FKBP12$^{f/f}$/αMyHC-Cre^{+} ventricular cardiomyocyte at 5 and 45 minutes into continuous dialysis with purified recombinant FKBP12 protein (1 μg/μl). **B**, I_{Na} remained unchanged in an FKBP12$^{f/f}$/αMyHC-Cre^{+} ventricular cardiomyocyte dialyzed with FKBP12-free pipette solution. **C**, Temporal changes in peak I_{Na} during continuous internal dialysis with FKBP12-containing and FKBP12-free, pipette solution, respectively. **D**, Normalized peak I_{Na}-V relationship at 5 and 45 minutes into FKBP12 dialysis. Internal perfusion of an FKBP12$^{f/f}$/αMyHC-Cre^{+} ventricular cardiomyocyte with FKBP12-free solution did not alter voltage-dependence of I_{Na} activation (not shown). **E,** Changes in voltage-dependence of I_{Na} activation and inactivation following FKBP12 application. **F**, The late I_{Na}/peak I_{Na} ratio is significantly increased following 45 minutes of FKBP12 dialysis. **G**, Representative action potential recordings over the course of FKBP12 dialysis. The arrow indicates the gradual prolongation of APD. H, Traces of dV/dt for the same action potentials shown in G. Traces were shifted along the time axis for display purposes.